# New Affine Projection Tanh-Based Algorithms for Active Impulsive Noise Control

Felix Albu
*Dept. of Electronics and Telecommunications*
*Valahia University of Targoviste*
Targoviste, Romania
felix.albu@valahia.ro

Ion Caciula
*Dept. of Electronics and Telecommunications*
*Valahia University of Targoviste*
Targoviste, Romania
ion.caciula@valahia.ro

Daniela Hagiescu
*R&D Department*
*Advanced Slisys SRL*
Bucharest, Romania
aslisys.121@gmail.com

***Abstract*— Two new affine projection and improved proportionate affine projection tanh-based algorithms for active impulsive noise control are presented. It is shown that they can obtain better performance for active impulsive noise control systems than the original algorithms when using a modified filtered-x (MFx) structure.**

***Keywords—affine projection tanh-based algorithms, modified filtered-x structure, active impulse noise control, proportionate-type algorithms.***

## I. INTRODUCTION

Active noise control (ANC) systems need to have a compact size and effective low-frequency noise reduction capabilities. In these systems, the active noise control algorithms generates anti-noise signals emitted through speakers to counter the unwanted noise [1]. They involve adaptive filters whose coefficients are iteratively adjusted. The filter generates a secondary sound with the same magnitude but with an opposite in phase to the primary noise[1]. It has been shown that the modified filtered-x (MFx) approach has a better convergence speed than the filtered-x approaches, although they have a higher numerical complexity too [1]-[3]. One of the most popular algorithms used in ANC systems is the affine projection (AP) algorithm [3]. The use of the improved proportionate principle of [4] has been previously proposed in [5]-[8] for applications such as echo cancellation or acoustic feedback cancellation. In order to improve the convergence properties of the above mentioned AP algorithms various evolutionary and variable step size strategies has been investigated [8]-[11]. However, impulsive noise often appears in real-time scenarios and the traditional ANC algorithms do not cope well in this case [1], [2]. The impulsive noise can have large value samples with a low probability (e.g. traffic noise, heavy industrial machinery, etc). The impulsive noise can cause temporary or permanent hearing loss, therefore, it is very important to develop efficient ANC algorithms and systems to cancel the impulsive noise. One of the simplest impulsive active noise control (IANC) systems use the filtered-x least mean square (FxLMS)-based variants [2]. However, it is known that the affine projection versions have better performances than the LMS-based algorithms for IANC [1].

In this paper, two new tanh-based versions of the affine projection and improved proportionate AP algorithms are proposed. The idea of recently proposed affine projection tanh algorithm (APTA) of [4] is adapted to the MFx structure and the MFx-APTA is proposed. Also, the proportionality priciple of [4] adapted to APTA (PAPTA) is combined with the MFx structure. Therefore, a novel modified filtered-x proportionate affine projection tanh algorithms (MFx-PAPTA) is also designed.

In Section II, a brief description of the proposed tanh-based multichannel modified filtered-x algorithm is presented. Simulations results are presented in Section III allowing the comparison of their performance and parameters influence. Finally, conclusions are summarized in Section IV.

## II. PROPOSED METHODS

The MFx structure from [10] is used. The AP algorithm is replaced by the proposed APTA or PAPTA. The multichannel APA equations for ANC with the MFx scheme is shown in Fig. 2 using the notations from Table 1 [10].

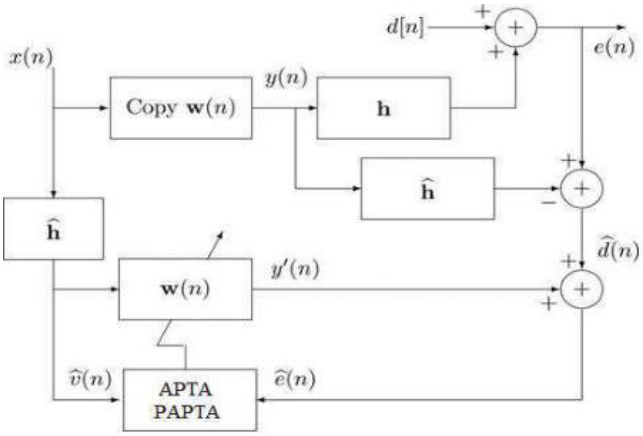


Fig. 1. Block diagram of an ANC system using the APTA/PAPTA with the modified filtered-x scheme

Require: $x_i(n)$ and $e_k(n)$

Ensure: Output $y_j(n)$

1: Update $\mathbf{x}_{Li}(n)$ and $\mathbf{x}_{Mi}(n)$

2: $y_j(n) = \sum_{i=1}^{I} \mathbf{w}_{ij}^T(n)\mathbf{x}_{Li}(n)$

3: $\hat{d}_k(n) = e_k(n) - \sum_{j=1}^{J} \mathbf{y}_j^T(n)\hat{\mathbf{h}}_{jk}$

4: $\hat{v}_{ijk}(n) = \mathbf{x}_{Mi}^T(n)\hat{\mathbf{h}}_{jk}$

5: $\hat{\mathbf{e}}_k(n) = \hat{\mathbf{d}}_k(n) + \sum_{i=1}^{I}\sum_{j=1}^{J} \hat{\mathbf{V}}_{ijk}^T(n)\mathbf{w}_{ij}(n)$

6: $\varepsilon_{ij}(n) = \sum_{k=1}^{K} \hat{\mathbf{V}}_{ijk}(n)\left[\hat{\mathbf{V}}_{ijk}^T(n)\hat{\mathbf{V}}_{ijk}(n) + \delta\mathbf{I}\right]^{-1}\hat{\mathbf{e}}_k(n)$

7: $\mathbf{w}_{ij}(n+1) = \mathbf{w}_{ij}(n) - \mu\varepsilon_{ij}(n)$

Fig. 2. The MFx-APA equations

Table 1 Notation of the MFx-APA [10]

| | |
|---|---|
| $I$ | Number of reference sensors |
| $J$ | Number of actuators |
| $K$ | Number of error sensors |
| $L$ | Length of the adaptive filters |
| $N$ | Projection order |
| $x_i(n)$ | $i$th reference signal at time $n$ |
| $y_j(n)$ | $j$th actuator signal at time $n$ |
| $e_k(n)$ | $k$th error sensor signal at time $n$ |
| $\hat{\mathbf{h}}_{jk}$ | Estimated FIR filter modeling the acoustic plant between the $k$th error sensor and the $j$th actuator |
| $\mathbf{w}_{ij}(n)$ | $\left[w_{ij1}(n), w_{ij2}(n), \ldots, w_{ijL}(n)\right]^T$ |
| $\mathbf{x}_{Li}(n)$ | $\left[x_i(n), x_i(n-1), \ldots, x_i(n-L+1)\right]^T$ |
| $\mathbf{x}_{Mi}(n)$ | $\left[x_i(n), x_i(n-1), \ldots, x_i(n-M+1)\right]^T$ |
| $\mathbf{y}_j(n)$ | $\left[y_i(n), y_i(n-1), \ldots, y_i(n-M+1)\right]^T$ |
| $\hat{\mathbf{v}}_{ijk}(n)$ | $\left[\hat{v}_{ijk}(n), \hat{v}_{ijk}(n-1), \ldots, \hat{v}_{ijk}(n-L+1)\right]^T$ |
| $\hat{\mathbf{d}}_k(n)$ | $\left[\hat{d}_k(n), \hat{d}_k(n-1), \ldots, \hat{d}_k(n-N+1)\right]^T$ |
| $\hat{\mathbf{V}}_{ijk}(n)$ | $\left[\hat{\mathbf{v}}_{ijk}(n), \hat{\mathbf{v}}_{ijk}(n-1), \ldots, \hat{\mathbf{v}}_{ijk}(n-N+1)\right]$ |

The step 6 of Fig. 2 of the proposed MFX-APTA using the notations from [10] is replaced with the following:

$$\boldsymbol{\varepsilon}_{ij}(n) = \sum_{k=1}^{K} \hat{\mathbf{V}}_{ijk}(n)\left[\hat{\mathbf{V}}_{ijk}^T(n)\hat{\mathbf{V}}_{ijk}(n) + \delta\mathbf{I}\right]^{-1} \tanh\left(\beta\hat{\mathbf{e}}_k(n)\right) \quad (1)$$

The update equation of the proposed MFX-PAPTA using the notations from [4] and [10] is:

$$\boldsymbol{\varepsilon}_{ij}(n) = \sum_{k=1}^{K} \mathbf{G}(n)\hat{\mathbf{V}}_{ijk}(n)\left[\hat{\mathbf{V}}_{ijk}^T(n)\mathbf{G}(n)\hat{\mathbf{V}}_{ijk}(n) + \delta_1\mathbf{I}\right]^{-1} \cdot \tanh\left(\beta\hat{\mathbf{e}}_k(n)\right), \quad (2)$$

where $\mathbf{G}(n)$ is a diagonal matrix containing the proportionate factors as follows:

$$g_l(n) = \frac{1-\alpha}{2LJ} + (1+\alpha)\frac{\left|w_{ij}(n)\right|}{2\left\|\mathbf{w}_{ij}(n)\right\|_1 + \theta}, \quad (3)$$

where $l = 0,1,\ldots,LJ-1$, $-1 \le \alpha < 1$, $\delta$ and $\delta_1$ are the regularization factors [4] and $\theta$ is a small constant.

## III. Simulation Results

The used impulsive noise has a Bernoulli-Gaussian (BG) distribution generated as a product of a Bernoulli process with a probability of success Pr = 0.001 and a Gaussian process keeping its average power constant [5]. For the multichannel case we have $I$ = 1, $J$ =3, $K$ =2, $L$ = 150, $\delta = 10^5$, $\alpha = 0$, $\theta = 10^{-6}$, and $\delta_1 = \delta(1-\alpha)/(2IJL)$ [4].

In Fig. 3 the convergence curves of the MFx-APTA with ideal plant models for ANC, $\mu = 1$, and five tanh parameter values are plotted in Fig. 3a, while for 10 dB noisy plant models are shown in Fig. 3b. It can be noticed that the best result is obtained for $\beta = 4$ in case of ideal plant models and for $\beta = 2$ in case of noisy plant models.

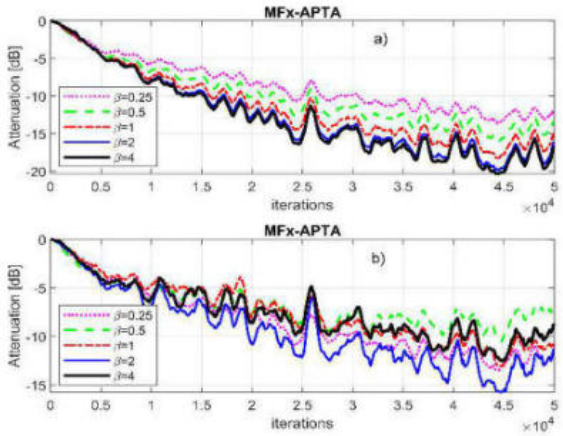


Fig. 3. Convergence curves of the multichannel modified filtered-x affine projection tanh algorithm for ANC, $N$ = 10, $\mu = 1$ and five tanh parameter values: a) ideal plant models; b) noisy plant models (10 dB).

In Fig. 4 the convergence curves of the MFx-PAPTA for ANC, $\mu = 1$, and five tanh parameter values are plotted for the ideal plant models (Fig. 4a) and for 10 dB noisy plant models (Fig. 4b).

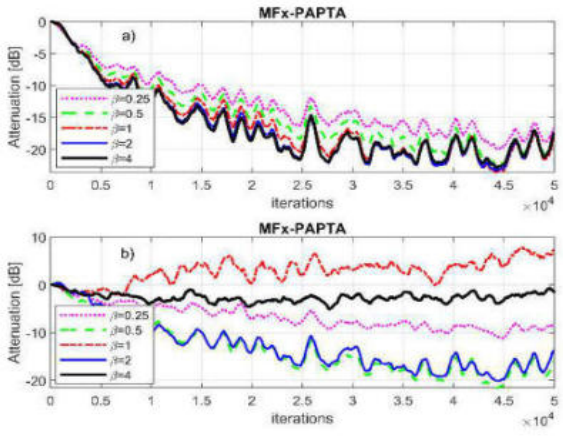


Fig. 4. Convergence curves of the multichannel modified filtered-x proportionate affine projection tanh algorithm for ANC, $N$ = 10, $\mu = 1$ and five tanh parameter values: a) ideal plant models; b) noisy plant models (10 dB).

The best attenuation performance is obtained for $\beta = 4$ for the ideal plant models. However, in case of the noisy plant

models, the best performance is obtained for $\beta = 0.5$, the attenuation being also smaller than that obtained when using the ideal plant models. It can be noticed from Fig. 4b that the stability of the MFx-PAPTA depends on the $\beta$ value when using noisy plant models. Also, by comparing performances from Figs. 3 and 4 it can be said that the MFx-PAPTA obtain a better performance than the MFx-APTA if a proper $\beta$ parameter is used.

In Fig. 5a the convergence curves of the MFx-APTA for ANC, with ideal plant models, $N = 10$, $\beta = 4$ and four step size values are plotted. It can be seen that the best results are obtained for $\mu = 1$. In Fig. 5b the convergence curves of the MFx-APTA for ANC, with noisy plant models (10 dB), $N = 10$, $\beta = 2$ and four step size values are shown. It can be noticed that the best results are obtained for $\mu = 0.75$.

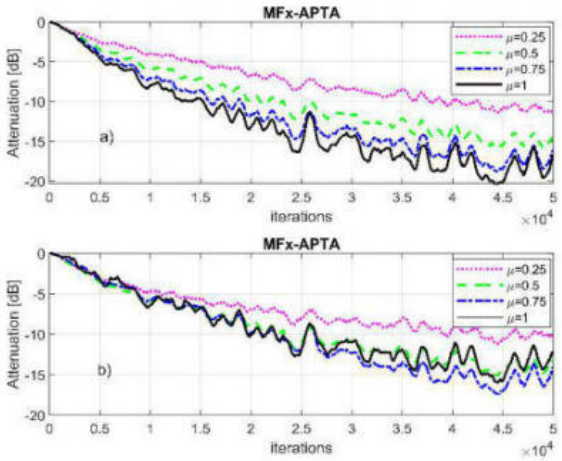


Fig. 5. Convergence curves of the multichannel modified filtered-x affine projection tanh algorithm for ANC, $N = 10$, and four step size values: a) $\beta = 4$, ideal plant models; b) $\beta = 2$, noisy plant models (10 dB).

In Fig. 6a the convergence curves of the MFx-PAPTA for ANC, with ideal plant models, $N = 10$, $\beta = 4$ and four step size values are plotted. In Fig. 6b the convergence curves of the MFx-PAPTA for ANC, with noisy plant models (10 dB), $N = 10$, $\beta = 0.5$ and four step size values are plotted. It can be seen that the best results are obtained for $\mu = 0.75$. Also, it can be noticed from Figs. 3-6 that the attenuation obtained with noisy plant models is smaller than that obtained with using ideal plant models.

The influence of the projection order for ideal and noisy path models is examined for MFx-APTA in Fig. 7 using the best parameters identified in Fig. 5. It is evident that increasing the projection order leads to improved attenuation properties in the case of ideal plant models.

The influence of the projection order for ideal and noisy path models is examined for MFx-PAPTA in Fig. 8 using the best parameters identified in Fig. 6. The same conclusions can be obtained regarding the projection order influence. Also, it can be deducted from Figs. 7 and 8 that the convergence properties of the MFx-PAPTA are generally better than those of the MFx-APTA for the same projection order.

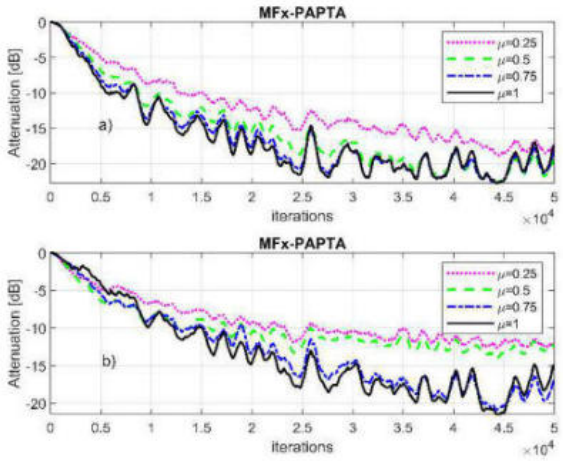


Fig. 6. Convergence curves of the multichannel modified filtered-x proportinate affine projection tanh algorithm for ANC, $N = 10$, and four step size values: a) $\beta = 4$, ideal plant models; b) $\beta = 0.5$, noisy plant models (10 dB).

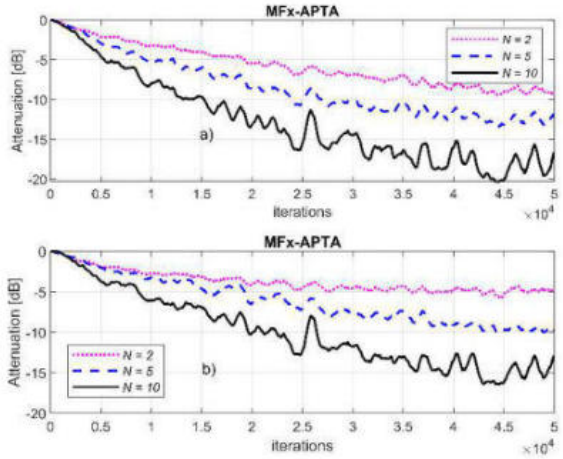


Fig. 7. Convergence curves for MFx-APTA, three projection order values and parameters from Fig. 5: a) ideal plant models; b) noisy plant models.

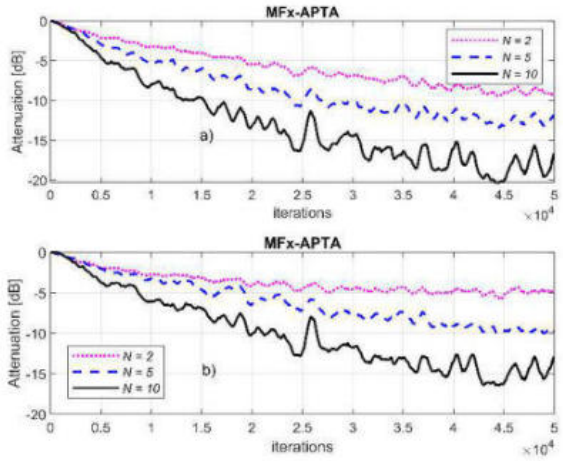


Fig. 8. Convergence curves for MFx-PAPTA, three projection order values and parameters from Fig. 6: a) ideal plant models; b) noisy plant models.

Figure 9 shows the attenuation curves in dB in case of impulsive noise input for the MFx-APA ($\mu = 1$), MFx-APTA and MFx-PAPTA for $N = 10$, and the parameters from previously reported best results. For the ideal plant models the

average improvement of the MFX-PAPTA over the original MFx-APA is around 9 dB and about 5 dB over the MFx-APTA. When using the 10 dB noisy plant models the average improvement of the MFX-PAPTA over the original MFx-APA decreases and it is around 6 dB and about 4 dB over the MFx-APTA. It can be noticed from Fig. 9 that the MFx-PAPTA has the best attenuation performance in both cased of plant models.

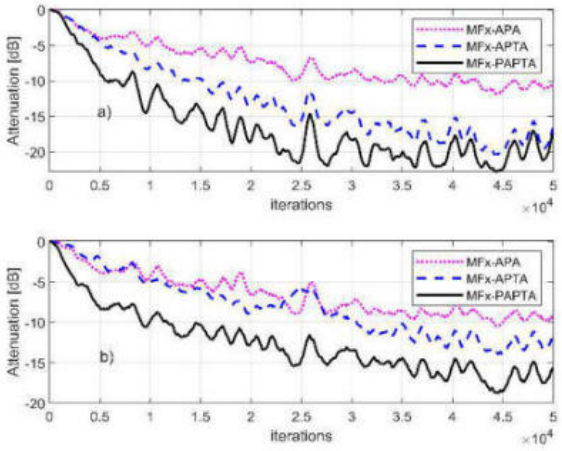


Fig. 9. Convergence curves of the MFx-APA, MFx-APTA and MFx-PAPTA for $N = 10$: a) ideal plant models; b) noisy plant models.

The added complexity of MFx-APTA over MFx-APA consists of $KN$ multiplications and $KN$ tanh operations. If $\beta$ is chosen as a power of two, $KN$ shift operations replaces the $KN$ multiplications. Therefore, the added complexity is minor because $N << L$. In addition to MFx-APTA, the MFx-PAPTA has 2 $LJ$ multiplications, $LJ$ additions and 2 divisions.

The future work will be focused on investigating the use of tanh-based noise reduction algorithms for nonlinear active noise control [13] and for tracking gait movements using inertial motion sensors [14]. It is expected that the increased robustness to outliers of the adapted tanh-based algorithms for the envisaged applications could improve their needed convergence characteristics.

## ACKNOLEDGMENT

This work was supported by a grant of the Ministry of Research, Innovation and Digitization, CNCS - UEFISCDI, project number PN-III-P4-PCE-2021-0780, within PNCDI and by the POSTUREC/121690 research project, co-financed through the POC 1.2.1-Innovative technological project program.

## IV. CONCLUSIONS

In this paper it is shown that the proposed tanh-based affine projection algorithms can provide improved robustness to impulsive noise. The influence of the step size and tanh parameter of the proposed MFx-APTA and MFx-PAPTA is examined through simulations for impulsive active noise control. With proper parameters, the proposed algorithms can provide good attenuation performance at a reasonable complexity for practical impulsive active noise control systems.

## REFERENCES

[1] Y. Liu and L. Zhichun Lei, "Review of Advances in Active Impulsive Noise Control with Focus on Adaptive Algorithms," Applied Sciences 14, no. 3: 1218, 2024.

[2] M.T. Akhtar, " An Adaptive Algorithm, based on Modified Tanh Non-linearity and Fractional Processing, for impulsive active noise control systems. J. Low Freq. Noise Vib. Act. Control 2018, 37, pp. 495–508.

[3] F. Albu, M. Bouchard, Y. Zakharov, "Pseudo Affine Projection Algorithms for Multichannel Active Noise Control", IEEE Transaction on Audio, Speech and Language Processing, Vol. 15, Issue 3, March 2007, pp. 1044-1052.

[4] J. Benesty and S. L. Gay, "An improved PNLMS algorithm," in Proc. of IEEE ICASSP 2002, pp. 1881–1884.

[5] F. Albu, H.K. Kwan, "Memory Improved Proportionate Affine Projection Sign Algorithm", IET Electronics Letters, October 2012, pp. 1279-1281.

[6] F. Albu, C. Paleologu, J. Benesty, and S. Ciochina, A low complexity proportionate affine projection algorithm for echo cancellation, in Proc. EUSIPCO, August 2010, pp. 6-10, 2010.

[7] F. Albu, C. R. C. Nakagawa, and S. Nordholm "Proportionate algorithms for two-microphone active feedback cancellation", in Proc. of EUSIPCO 2015, pp. 290-294.

[8] H. Li, J. Ni, "Proportionate affine projection tanh algorithm and its step-size optimization," Signal Processing, October 2024

[9] F. Albu, C. Paleologu, S. Ciochina "New variable step size affine projection algorithms", in Proc. of COMM 2012, Bucharest, Romania, pp. 63-66.

[10] A. Gonzalez, F. Albu, M. Ferrer, and M. de Diego, "Evolutionary and variable step size strategies for multichannel filtered-x affine projection algorithms," IET Signal Process., vol. 7, no. 6, pp. 471–476, Aug. 2013.

[11] F. Albu, C. Paleologu, J. Benesty, "A Variable Step Size Evolutionary Affine Projection Algorithm", in Proc. of ICASSP 2011, Prague, Czech Republic, May 2011, pp. 429-432.

[12] Q. Zhang, S. Wang, D. Lin, and S. Chen, "Robust Affine Projection Tanh Algorithm and Its Performance Analysis," Signal Processing, vol 202, 2023.

[13] Y. Xiao, S. Chen, Q. Zhang, D. Lin, M. Shen, J. Qian, and S. Wang, "Generalized hyperbolic tangent based random Fourier conjugate gradient filter for nonlinear active noise control," IEEE/ACM Trans. Audio, Speech, Language Process., vol. 31, pp. 619–632, 2023.

[14] F. Ohberg, R. Lundstrom and H. Grip, "Comparative analysis of different adaptive filters for tracking lower segments of a human body using inertial motion sensors", Meas. Sci. Technol. 24, 2013.